Biosensors and Bioelectronics 66 (2015) 399–404

Contents lists available at ScienceDirect

Biosensors and Bioelectronics

journal homepage: www.elsevier.com/locate/bios

Enzyme-free and label-free fluorescence sensor for the detection of liver cancer related short gene

Xianghui Li [a,1], Longjie Gan [b,1], Qishui Ou [a,b], Xi Zhang [c], Shuxian Cai [c], Dongzhi Wu [c], Mei Chen [c], Yaokun Xia [c], Jinghua Chen [c,*], Bin Yang [b,*]

[a] Medical Technology and Engineering College, Fujian Medical University, Fuzhou 350004, Fujian, China
[b] Department of Laboratory Medicine, The 1st Affiliated Hospital of Fujian Medical University, 20 Chazhong Road, Fuzhou 350004, Fujian, China
[c] Department of Pharmaceutical Analysis, Faculty of Pharmacy, Fujian Medical University, Fuzhou 350108, Fujian, China

ARTICLE INFO

Article history:
Received 27 August 2014
Received in revised form
25 November 2014
Accepted 26 November 2014

Keywords:
G-quadruplex
Enzyme-free
Label-free
Thioflavine T
Fluorescence sensor

ABSTRACT

Non-invasive early diagnosis of liver cancer is the most effective way to improve the survival rate. In this paper, we developed a label-free and enzyme-free fluorescent biosensor based on target recycling and Thioflavin T (ThT) induced G-quadruplex formation for MXR7 (liver cancer related short gene) detection in human serum. The proposed sensor can detect the target DNA in the concentration range of 0–350 fM with the detection limit as low as 10 fM. Due to the outstanding structural selectivity of ThT for G-quadruplex, this sensor possesses better discrimination ability and higher sensitivity. Furthermore, this enzyme-free and label-free fluorescence sensor has demonstrated to be capable of detecting target DNA in human serum samples because of its high selectivity and sensitivity. The mechanism employed in this study represents a promising path toward directing liver cancer detection in human serum. In addition, this strategy may be extended to detect other cancer related genes by choosing a rational DNA probe according to different sequences of targets.

1. Introduction

Liver cancer, as a lethal disease, is one of the most common cancers worldwide with the rising morbidity year by year (Llovet and Bruix, 2008). Accurate diagnosis of liver cancer is important to determine the extent of disease and to plan appropriate therapies. Especially, the early diagnosis of liver cancer is of great significance for improving the survival rate via early treatment and reducing the suffering and cost for the patients. At present, the conventionally used clinical diagnosis methods for liver cancer are ultrasound elastograph (Kudo, 2014), computed tomography (CT) (Sofocleous et al., 2014), liver puncture needle aspiration cytology (Novak et al., 2014), etc. However, these universal methods have the following drawbacks, damage to patient body, time-consuming, high cost, etc. Tumor markers existing in tumor cells or host body fluids are substances which can be used for diagnosis of tumors based on their biochemical or immune characteristics (Lai et al., 2012). The accurate detection of tumor markers in biosamples has been regarded as an ideal method in early stage due to its higher sensitivity, non-invasiveness, simplicity and low cost. Some tumor markers are always used to evaluate specific cancers, but most are less predictable. For example, an elevation of alpha-fetoprotein (AFP) level in human serum can indicate not only liver cancer but also epithelial ovarian tumors, which bring substantial difficulty for the diagnosis of liver cancer. Hence, it is necessary to explore a more credible and specific diagnostic marker of hepatocellular tumor. Recently, the mitoxantrone resistance7 (MXR7) oncogene has been recognized as an efficient early marker of liver carcinogenesis with great applied prospect (Wang et al., 2006).

The fluorescent biosensor has been proved to be a promising tool for clinical diagnosis owing to its appealing advantages (Chung et al., 2009). However, because of the low concentration of MXR7 and complex background of serum, conventional fluorescent biosensors cannot be available to meet the clinical diagnostic requirement for direct MXR7 detection in human serum. To address this problem, many enzyme-based amplification approaches had been developed (Fu et al., 2011; Weizmann et al., 2006; Wang et al., 2011; Tian et al., 2006; Cheglakov et al., 2007; Cheglakov et al. 2006). However, the applications of these amplified sensors are restricted by the fact that protein enzymes are of high-cost and the enzymatic activity is sensitive to reaction conditions (Zheng et al., 2012). Thus, several enzyme-free sensors have been also proposed based on hybridization and strand displacement (Dirks and Pierce, 2004; Huang et al., 2011; Wang et al., 2011; Zhang et al., 2007; Bi et al., 2011; Yin et al., 2008; Li et al.,

* Corresponding authors. Fax: +86 591 83340702.
E-mail addresses: cjh_huaxue@126.com (J. Chen), yangbin607@163.com (B. Yang).
[1] Both Xianghui Li and Longjie Gan are the first authors.

http://dx.doi.org/10.1016/j.bios.2014.11.049
0956-5663/

2011). But these approaches always require specific labels or extra steps to obtain optical or electrochemical signals, which makes them time-consuming or high-cost (Lu et al., 2010). So the development of label-free and enzyme-free methods is a necessity for such amplified sensors to realize their extensive practical application and biomedical utilization in DNA detection.

In this study, an enzyme-free and label-free fluorescence sensor for liver cancer related short gene (MXR7) has been developed. The proposed sensor has been applied to detect the target in the human serum samples with satisfied results. Hence, this study may provide an approach for liver cancer detection, which may also be extended to detect other cancers in the near future.

2. Experimental

2.1. Reagents and apparatus

All the designed DNA sequences in this study were synthesized by Sangon (Shanghai, China), purified by high-performance liquid chromatography (HPLC), and confirmed by mass spectrometry (MS). The concentrations were quantified by OD 260 based on their individual absorption coefficients. Each DNA was heated to 90 °C for 5 min and was slowly cooled down to room temperature before use. The sequences of oligonucleotides used in this study are list as follows:

Hairpin 1 (H1): 5′-**GGG TAG GGC GGG TTG GG** AT *TAG GAA AGG CTG CCA* CATCC CAA CCC ATA-3′
Hairpin 2 (H2): 5′-TATGGG TTGGGATGTGGCAGCCATCCCAAC-3′
Perfectly complementary target (T1, MXR7): 5′-TGGCAGCC TTTCCTA-3′
Single-base-mismatched target (T2): 5′-TGGCAGCGTTTCCTA-3′
Double-base-mismatched target (T3): 5′-TGGCAGGCATTCCTA-3′
Three-base mismatched target (T4): 5′-TGCCAGGCTTTCGTA-3′
Non-complementary target (T5): 5′-ACCATCGGAAAGGAT-3′

The boldfaced letters indicate the sequence that forms a G-quadruplex; the italic letters are the complementary sequence of T1; the underlined letters are the mismatched base sequence.

ThT (3,6-dimethyl-2-(4-dimethylaminophenyl)benzo-thiazoliumcation), obtained from Sigma-Aldrich, was purified by column chromatography using a silica gel column and mildly acidic methanol as the eluent. All other chemicals were purchased from Sigma-Aldrich and used without further purification. The water used was obtained by purification of distilled water with a Millipore Milli-Q system. All measurements were performed in reaction buffer (50 mM Tris–HCl, 50 mM KCl, 10 mM $MgCl_2$, pH 7.5) unless otherwise stated.

The human serum samples of liver cancer patients (confirmed by pathological examinations) were obtained from the First Affiliated Hospital of Fujian Medical University (Fujian, China).

Fluorescence spectra (Varian Cary Eclipse Fluorimeter, Varian, Inc., Agilent Technologies) were measured with a Peltier block, using quartz fluorescence cuvettes (4 mm × 10 mm, Sub-micro, 50 μL), and with the following settings: λ_{ex}=441 nm, λ_{em} =485 nm, 5 nm slit, PMT detector voltage=650 V. UV–vis absorbance spectra were measured with a UV-2501 PC spectrophotometer (SHIMADZU, Japan) using a quartz cell with 1.0 cm optical pathway. The circular dichroism (CD) spectra were studied based on a JascoJ-810 CD spectropolarimeter (Tokyo, Japan). The optical chamber (1 cm path length, 500 μL volume) was deoxygenated with dry purified nitrogen (99.99%) before use and kept in the nitrogen atmosphere during experiments. Three scans (100 nm min^{-1}) from 220 nm to 330 nm at 0.1 nm intervals were accumulated and averaged. The background of the buffer solution was subtracted from the CD data.

2.2. Preparation of the fluorescent biosensor for T1 detection

Different concentrations of T1 were mixed and reacted with 50 μL of reaction buffer containing 200 nM H1, 300 nM H2, and 3 μM ThT at 38 °C for 2 h, respectively. The fluorescence spectra of the above resulted solutions were recorded in the wavelength range from 445 nm to 580 nm with the excitation of 441 nm at room temperature.

2.3. Preparation of human serum sample

The human serum samples were centrifuged at 603*g* for 10 min at 4 °C. Then, the 1 mL of supernatant liquid was taken and diluted to 100 mL with buffer solution. The different concentrations of T1 were then added into the diluted serum to prepare artificial serum samples and the concentrations of T1 in the samples were determined with our biosensor.

3. Results and discussion

3.1. Principle of the biosensor

It has been reported that the G-rich nucleic acid sequences under certain conditions can form G-quadruplexes, which are unique higher-order structures of stacked arrays of G-quartets connected by Hoogsteen-type base pairing (Phan et al., 2006; Amrane et al., 2009; Kong et al., 2009). Water soluble ThT is weakly fluorescent by itself, but can exhibit greatly enhanced fluorescence upon inducing DNA folding into G-quadruplex under physiological salt conditions, which owns pronounced structural selectivity for G-quadruplexes but not for single, double or triplexes stranded DNA. (Mohanty et al., 2013) This character is applied to design the sensitive fluorescence sensor for MXR7 in this study. As shown in Fig. 1, this DNA detection system contains ThT and two hairpin DNAs (hairpins) termed as H1 and H2. H1 contains three domains termed as 1, 2, and 3, while H2 contains two domains termed as regions 4 and 5. The region 3 of the partially oligonucleotides of H1 is guanine-rich sequence (G-rich sequence). In addition, the region 2 is complementary to the target MXR7 (T1), and the region 4 is complementary to region 1 and 2. Thus, in the presence of target MXR7, the region 2 of H1 will hybridize with the target, leading to the release of regions 1 and 3. When both H1 and H2 exist at the same time, the target is replaced with the sequence 4 of H2 because the region 4 can form more stable DNA structure with the regions 1 and 2. Subsequently, the released target further hybridizes with another H1, which induces the cycling of G-rich sequence folding into quadruplex. After numerous cycles, all regions 3 of the H1 hairpins are released, and then fold into quadruplex and bind with ThT, resulting in obvious enhancement of the fluorescent signal. Herein, an enzyme-free and label-free fluorescence sensor for DNA detection is developed.

3.2. Optimization of experimental conditions

To achieve the best sensing performance of the fluorescence sensor, the main experimental variables, such as hybridization temperature, concentration of ThT, incubation time and pH, were optimized (as shown is Fig. 2). The temperature of the detection system is a key factor which directly affects the hybridization efficiency of H1/H2/T1. Hence, the temperature was firstly investigated. As shown in Fig. 2A, with the rise of the hybridization temperature, the fluorescence intensity increases firstly and then

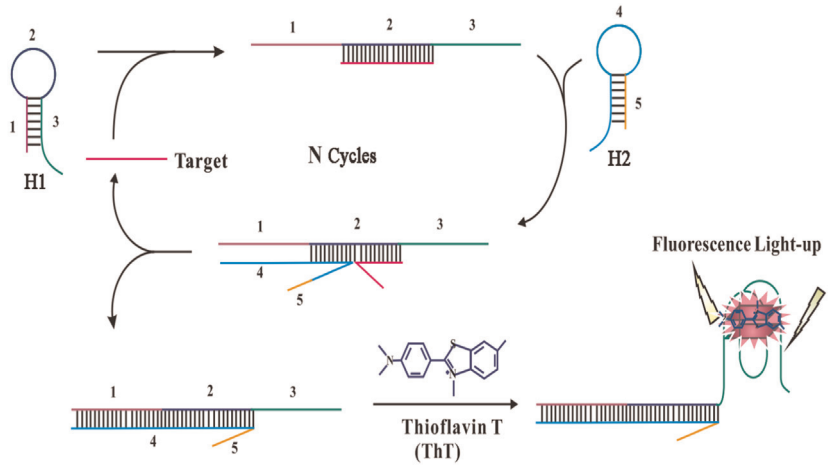

Fig. 1. Schematic illustration of the fluorescence sensor for the detection of liver cancer related short gene (MXR7).

decreases. Considering the fact that the theoretical hybridization temperature of DNA is about 40 °C and the fluorescence intensity is the highest around 38 °C, 38 °C is selected for subsequent experiments.

Besides, the ThT concentration is also vital for this experiment. Thus, measurements in the presence of different concentrations of ThT displayed remarkable changes. As depicted in Fig. 2B, it is obvious that the optimum ThT concentration is 3 μM according to the best signal of this system.

The fluorescence intensity can be influenced by the incubation time as well. As shown in Fig. 2C, the fluorescence intensity reaches a stable value when the reaction time exceeds 50 min, so the optimal time (50 min) was chosen for further studies. At last, the effect of pH of the buffer on the fluorescence intensity is examined. The result shown in Fig. 2D indicates that the optimal pH of buffer is 7.5.

3.3. Identification of quadruplex formation by circular dichroism

Circular dichroism (CD) is one helpful tool for detection and characterization of DNA structures, including dsDNA and G-quadruplex species. Hence, the CD spectra were also applied to assess the feasibility of our strategy. As shown in Fig. 3, the CD spectra of H1, H2, and H1+H2, exhibit a positive peak at about 270 nm and a negative peak at around 240 nm owing to the base stacking and the helicity, respectively. It is noted that the intensity of the CD spectrum greatly increases with the simultaneous presence of H1 and H2, indicating that the structures of H1 and H2 hardly change. However, the CD spectrum is dramatically changed after the addition of T1. To be specific, a characteristic positive peak for anti-parallel G-quadruplex (Balagurumoorthy and Brahmachari, 1994) emerges at about 300 nm while the initial band

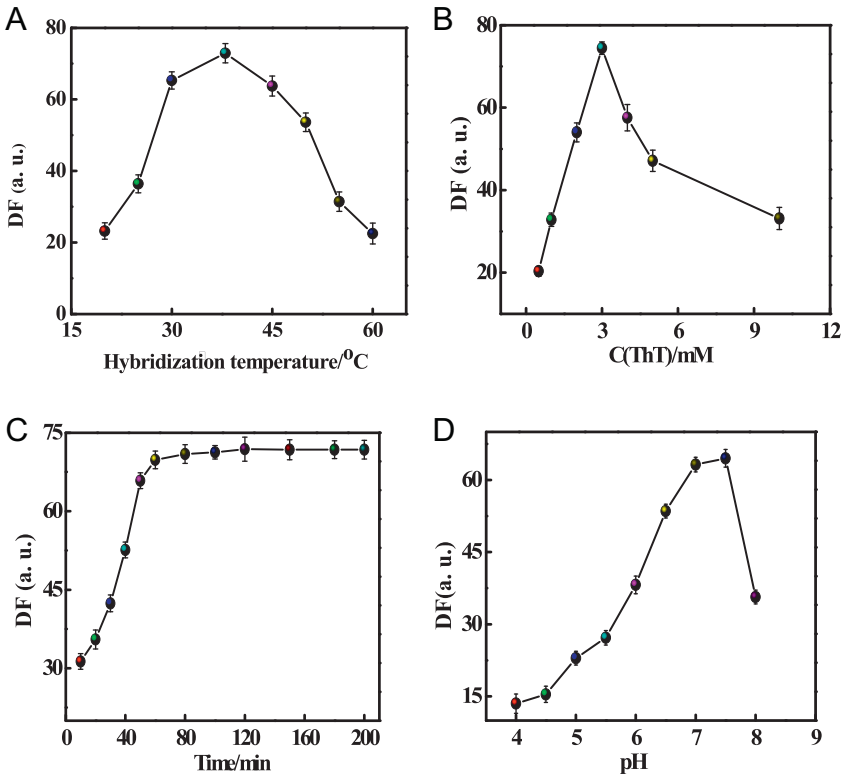

Fig. 2. Influence of the hybridization temperature (A), the concentration of ThT (B), the incubation time (C) and pH (D) on the fluorescence intensity. Each data point represents the average value of three independent experiments with error bars indicated.

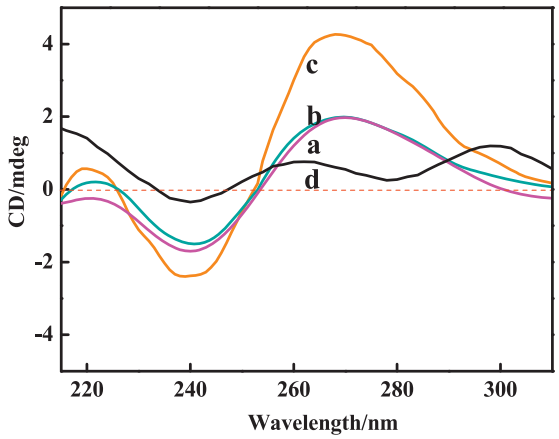

Fig. 3. CD spectra of H1 (a), H2 (b), H1+H2 (c), and H1+H2+T (d) in reaction buffer.

near 270 nm of H1+H2 decreases obviously. This phenomenon reveals that the cyclicprocess of this fluorescence sensor is initiated and the sequences 3 are released as typical anti-parallel G-quadruplex conformations in the presence of ThT and monovalent ions.

3.4. Identification of quadruplex formation by UV–vis and fluorescent spectra

To further validate the feasibility of our sensor, the UV–vis spectra were used to investigate absorbance changes of this detection system. As shown in Fig. 4A, in dilute solution of ThT (3 μM) reaction buffered at pH 7.5, the ThT dye displays its characteristic absorption profile with a maximum at 412 nm (curve a). Upon the addition of H1, H2, H1+H2 (curves b, c, and d, respectively), an obvious hypochromism can be observed. In this system, both H1 and H2 are hairpin DNA. Meanwhile, the subsistent structures are the negatively charged phosphate groups. With the presence of the positively charged groups of the ThT, there is an electrostatic interaction between DNA and ThT. However, an obvious red-shift (the absorption peak at 412 nm shifts to 445 nm) is observed in the present of coexistent H1, H2 and liver cancer related short gene (T1) (curve e), implying the corresponding changes of DNA conformation and structure. Since the binding sites of ThT in the G-quadruplexes are more specific and rigid, a remarkable red-shift in the UV–vis spectrum is observed here (Mohanty et al. 2013). Hence, all the UV–vis results mentioned above also validate that the proposed fluorescence sensor can work well as we expect.

Moreover, the fluorescence measurements were also carried out to test the principle of our designed sensor. As can be seen from Fig. 4B, the ThT exhibits a very weak fluorescence emission. The fluorescence intensities of the samples containing H1, H2, and H1+H2 are close to that of ThT, implying that no ThT responsive G-quadruplex formed in these samples (curves b, c, and d, respectively). However, upon the simultaneous addition of H1, H2 and T1, an extraordinary fluorescence enhancement can be realized (curve e). These results demonstrate that the T1 is a trigger of the cyclic unfolding progress of H1, providing many released sequences 3 of H1 to fold into G-quadruplexes. The binding sites in the G-quadruplexes are specific and rigid for ThT, and thereby the fluorescence intensity increases dramatically. Consequently, the above fluorescence results again confirm the feasibility of the proposed biosensor.

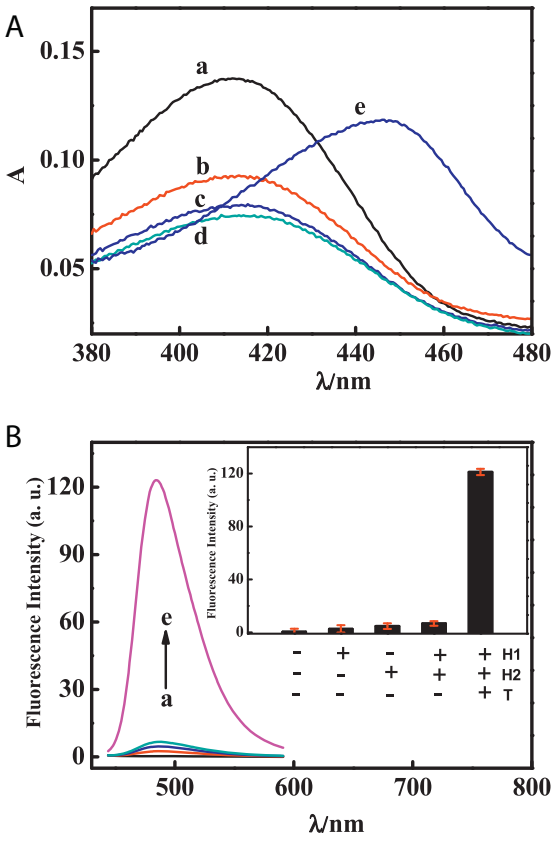

Fig. 4. (A) UV–vis spectra of 3 μM ThT (a) in the presence of 10 μM H1 (b), H2 (c), H1+H2 (d), and H1+H2+T (e), in reaction buffer with 50 mM Tris (pH 7.5) and 50 mM KCl, respectively. (B) It is the fluorescence spectra of 3 μM ThT (a) in the presence of 10 mM H1 (b), H2 (c), H1+H2 (d), H1+H2+T (e) in the same reaction buffer, respectively.

3.5. Sensitivity of the biosensor

To evaluate the sensitivity of the proposed fluorescent biosensor, fluorescence spectra at varying concentrations of MXR7 (T1) were recorded under the optimized assay conditions. The results were shown in Fig. 5. It can be clearly observed that the fluorescence intensity markedly increases with increasing T1 concentration. It can be explained by the reason that more T1 added, more G-quadruplex formed, resulting in the remarkable enhancement of fluorescence intensity. Besides, it is worth noting that the fluorescence intensity of this system is linear to the concentration of T1 ranging from 0 fM to 350 fM (see Fig. 5, inset)

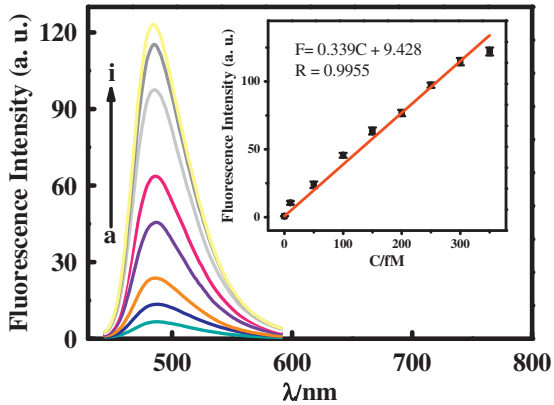

Fig. 5. ThT+H1/H2 in the presence of various concentrations of perfectly matched target DNA (from a to i: 0.00, 10 fM, 50 fM, 100 fM, 150 fM, 200 fM, 250 fM, 300 fM, and 350 fM, respectively).

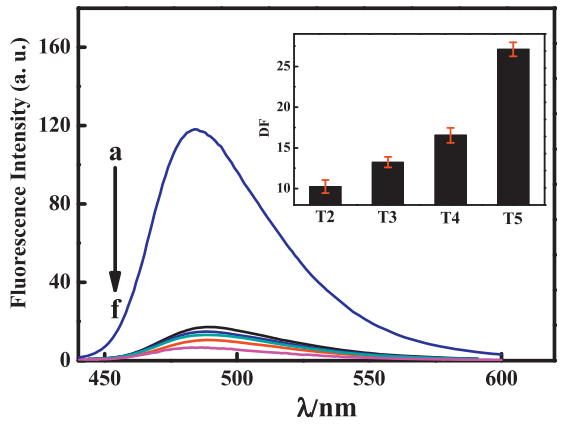

Fig. 6. Specificity of the DNA assay detecting different targets: T1 (a), T2 (b), T3 (c), T4 (d), T5 (e), and no target DNA was added (f). The illustration is the DF obtained with different sequences: T2 (a), T3 (b), T4 (c), and T5 (d). The concentrations of T2, T3, T4 and T5 were all 1 pM.

with a detection limit of 10 fM. The linear regression equation can be expressed as

$$F = 0.339C_T + 9.428(R = 0.9955) \quad (1)$$

where F is the fluorescence intensity at 485 nm, C_T represents the concentration of T1, and R is the regression coefficient.

Compared with previously reported biosensors, the detection limit of this proposed biosensor is lower than 20 fM with the label-free fluorescent biosensor detecting short DNA species of c-erbB-2 in saliva (Chen et al., 2014) and 0.1 pM with the enzyme-free DNAzyme sensor based on target-catalyzed hairpin assembly (Zheng et al., 2012). These demonstrate that our designed fluorescent biosensor is highly sensitive.

3.6. Selectivity of the proposed sensor

Fig. 6 displays the observed fluorescence intensity upon addition of different targets, i.e., T1, T2, T3, T4, T5 and no target DNA. An obvious fluorescence enhancement can be seen with the addition of T1 (curve a), while sharply decreased fluorescence intensities are obtained with the other targets (T2, T3, and T4, indicated as curves b, c, and d, respectively). Especially, it shows that non-complementary T5 DNA (curve e) has nearly no response, similar to the blank controller (curve f).

To clarify the discrimination ability of this fluorescence sensor, the discrimination factor (DF) (defined as $(F2-F0)/(F1-F0)$, where F1, F2, and F0 are the fluorescence intensities produced by the addition of complementary target (T1), mismatched target (T2–T5) and the background (without target), respectively) has been studied. The smaller DF indicates the higher specificity. As can be seen from Fig. 6, the fluorescence intensity of T1 is higher than those of other mismatched DNA sequences, and the inserted histogram also clearly confirms the same verdict. The DF of T5 is the highest with a value of 27.1, while the DF values of T2, T3, and T4 are 10.3, 13.2, and 16.5, respectively.

Furthermore, the selectivity of this proposed sensor has been also compared with those of previous fluorescent and electrochemical biosensors. Due to the high selectivity of ThT for G-quadruplex, our sensor possesses better discrimination ability even against single-base mismatch. The detailed comparison has been summarized in Table S1 in the Supplementary material.

3.7. Detection of real sample

In order to indentify the practicability of this developed strategy in detecting targets in complex real biological samples, different concentrations of T1 have been added in human serum samples and then been detected by the proposed sensor. Herein, the human serums were obtained from the First Affiliated Hospital of Fujian Medical University, and diluted in 1% with Tris–HCl buffer and injected with the T1 at three concentrations (50, 100 and 250 fM) prior to measuring. The result is presented in Table S2 in the Supplementary material. From Table S2, it can be seen clearly that our method exhibits the acceptable recovery rates of standard addition from 96% to 104%, demonstrating that this proposed sensor has substantial potential in clinical diagnosis of liver cancer.

4. Conclusions

Based on ThT and G-quadruplex DNA structure, a simple, label-free and enzyme-free, ultra-highly sensitive and selective fluorescent biosensor for detection of liver cancer related short gene was developed. The proposed sensor can detect T1 in concentration as low as 10 fM, which is better than previously reported assay systems. The excellent sensitivity of this biosensor sensor originated from the target assisted recycling and the outstanding structural selectivity of ThT for G-quadruplex in DNA amplification techniques. Herein, the formation of G-quadruplex was identified by CD, UV–vis and fluorescent spectra. Due to the high selectivity of ThT for G-quadruplex, this sensor possesses better selectivity compared with previous fluorescent and electrochemical biosensors. Finally, the practical application was performed using a series of human serum samples mixed with different concentrations of target. As more and more tumor markers have been found up to now, this study may provide new insights into the detection of other cancer related short genes by choosing a rational DNA probe on the basis of different sequences of targets.

Acknowledgements

The authors gratefully acknowledge the financial support of National Natural Science Foundation of China (21375017, 21105012, 21205015), National Science Foundation for Distinguished Young Scholars of Fujian Province (2013J06003), the Key Project of Fujian Science and Technology (2013Y0045), Program for New Century Excellent Talents of Colleges and Universities in Fujian Province (JA13130, JA13088), Program for Fujian University Outstanding Youth Scientific Research (JA11105, JA10295), the Foundation of Fuzhou Science and Technology Bureau (2013-S-122-4), Medical Elite Cultivation Program of Fujian, P. R.C (2014-ZQN-ZD- 26). Doc. Fang Luo at University of South Australia is thanked for assistance with the English in this paper.

Appendix A. Supplementary Information

Supplementary data associated with this article can be found in the online version at http://dx.doi.org/10.1016/j.bios.2014.11.049.

References

Amrane, S., Ang, R.W., Tan, Z.M., Li, C., Lim, J.K., Lim, J.M., Lim, K.W., Phan, A.T., 2009. Nucleic Acids Res. 37, 931–938.
Bi, S., Zhang, J., Hao, S., Ding, C., Zhang, S., 2011. Anal. Chem. 83, 3696–3702.

Balagurumoorthy, P., Brahmachari, S.K., 1994. J. Biol. Chem. 269, 21858–21869.
Chung, S.Y., Nam, S.W., Lim, J., Park, S., Yoon, J., 2009. Chem. Commun. 20, 2866–2868.
Cheglakov, Z., Weizmann, Y., Basnar, B., Willner, I., 2007. Org. Biomol. Chem. 5, 223–225.
Cheglakov, Z., Weizmann, Y., Beissenhirtz, M.K., Willner, I., 2006. Chem. Commun. 30, 3205–3207.
Chen, J., Lin, J., Zhang, X., Cai, S., Wu, D., Li, C., Yang, S., Zhang, J., 2014. Anal. Chim. Acta, 817.
Dirks, R.M., Pierce, N.A., 2004. Proc. Natl. Acad. Sci. USA 101, 15275–15278.
Fu, R., Li, T., Lee, S.S., Park, H.G., 2011. Anal. Chem. 2011 (83), 494–500.
Huang, J., Wu, Y., Chen, Y., Zhu, Z., Yang, X., Yang, C.J., Wang, K., Tan, W., 2011. Angew. Chem. Int. Ed. 50, 401–404.
Kudo, M., 2014. Liver Cancer 3 (1), 1–5.
Kong, D.M., Ma, Y.E., Wu, J., Shen, H.X., 2009. Chem. Eur. J. 15, 901–909.
Llovet, J.M., Bruix, J., 2008. J. Hepatol. 48 (Suppl. 1), S20–S37.
Lai, W., Zhuang, J., Tang, J., Chen, G., Tang, D., 2012. Microchim. Acta 178, 357–365.
Li, B., Ellington, A.D., Chen, X., 2011. Nucleic Acids Res. 39, e110.
Lu, C.H., Li, J., Liu, J.J., Yang, H.H., Chen, X., Chen, G.N., 2010. Chem. Eur. J. 16, 4889–4894.
Mohanty, J., Barooah, N., Dhamodharan, V., Harikrishna, S., Pradeepkumar, P.I., Bhasikuttan, A.C., 2013. J. Am. Chem. Soc. 135, 367–376.
Novak, A., Olson, M., Ali, S., VandenBussche, C., 2014. J. Am. Soc. Cytopathol. 3 (5), S 74.
Phan, A.T., Kuryavyi, V., Patel, D.J., 2006. Curr. Opin. Struct. Biol. 16, 288–298.
Sofocleous, C.T., Garcia, A.R., Pandit-Taskar, N., Do, K.G., Brody, L.A., Petre, E.N., Capanu, M., Longing, A.P., Chou, J.F., Carrasquillo, J.A., Kemeny, N.E., 2014. Clin. Colorectal Cancer 13 (1), 27–36.
Tian, Y., He, Y., Mao, C., 2006. ChemBioChem 7, 1862–1864.
Wang, X.Y., Degos, F., Dubois, S., Tessiore, S., Allegretta, M., Guttmann, R.D., Jothy, S., Belghiti, J., Bedossa, P., Paradis, V., 2006. Hum. Pathol. 37 (11), 1435–1441.
Weizmann, Y., Beissenhirtz, M.K., Cheglakov, Z., Nowarski, R., Kotler, M., Willner, I., 2006. Angew. Chem. Int. Ed. 45, 7384–7388.
Wang, H.Q., Liu, W.Y., Wu, Z., Tang, L.J., Xu, X.M., Yu, R.Q., Jiang, J.H., 2011. Anal. Chem. 83, 1883–1889.
Wang, F., Elbaz, J., Orbach, R., Magen, N., Willner, I., 2011. J. Am. Chem. Soc. 133, 17149–17151.
Yin, P., Choi, H.M.T., Calvert, C.R., Pierce, N.A., 2008. Nature 451, 318–322.
Zheng, A.X., Li, J., Wang, J.R., Song, X.R., Chen, G.N., Yang, H.H., 2012. Chem. Commun. 48, 3112–3114.
Zhang, D.Y., Turberfield, A.J., Yurke, B., Winfree, E., 2007. Science 318, 1121–1125.